Journal of Theoretical Biology 319 (2013) 50–61

Contents lists available at SciVerse ScienceDirect

Journal of Theoretical Biology

journal homepage: www.elsevier.com/locate/yjtbi

Developing a temperature-driven map of the basic reproductive number of the emerging tick vector of Lyme disease *Ixodes scapularis* in Canada

Xiaotian Wu [a,b], Venkata R. Duvvuri [a], Yijun Lou [c], Nicholas H. Ogden [d,*], Yann Pelcat [e], Jianhong Wu [a,b]

[a] Centre for Disease Modelling, York Institute of Health Research, Toronto, Ontario, Canada
[b] Mathematics and Statistics, York University, Toronto, Ontario, Canada
[c] Department of Applied Mathematics, The Hong Kong Polytechnic University, Hung Hom, Kowloon, Hong Kong
[d] Zoonoses Division, Centre for Food-Borne, Environmental and Zoonotic Infectious Diseases, Public Health Agency of Canada, Saint-Hyacinthe, Quebec, Canada
[e] Population and Environmental Determinants Division, Laboratory for Foodborne Zoonoses, Public Health Agency of Canada, Saint-Hyacinthe, Quebec, Canada

HIGHLIGHTS

- A deterministic model of the Lyme disease vector, *I. scapularis*, was developed.
- The model was used to estimate $\mathcal{R}_0$ for *I scapularis* under different climatic conditions.
- A map of $\mathcal{R}_0$ was developed for *I scapularis* in Canada, where this tick is emerging.
- Estimation of $\mathcal{R}_0$ for *I. scapularis* will assist public health responses to emerging Lyme disease.

ARTICLE INFO

Article history:
Received 7 June 2012
Received in revised form
7 November 2012
Accepted 12 November 2012
Available online 1 December 2012

Keywords:
Lyme
Tick
Climate
Mapping

ABSTRACT

A mechanistic model of the tick vector of Lyme disease, *Ixodes scapularis*, was adapted to a deterministic structure. Using temperature normals smoothed by Fourier analysis to generate seasonal temperature-driven development rates and host biting rates, and a next generation matrix approach, the model was used to obtain values for the basic reproduction number ($\mathcal{R}_0$) for *I. scapularis* at locations in southern Canada where the tick is established and emerging. The $\mathcal{R}_0$ at Long Point, Point Pelee and Chatham sites where *I. scapularis* are established, was estimated at 1.5, 3.19 and 3.65, respectively. The threshold temperature conditions for tick population survival ($\mathcal{R}_0 = 1$) were shown to be the same as those identified using the mechanistic model (2800–3100 cumulative annual degree days $> 0\,^{\circ}$C), and a map of $\mathcal{R}_0$ for *I. scapularis*, the first such map for an arthropod vector, was drawn for Canada east of the Rocky Mountains. This map supports current risk assessments for Lyme disease risk emergence in Canada. Sensitivity analysis identified host abundance, tick development rates and summer temperatures as highly influential variables in the model, which is consistent with our current knowledge of the biology of this tick. The development of a deterministic model for *I. scapularis* that is capable of providing values for $\mathcal{R}_0$ is a key step in our evolving ability to develop tools for assessment of Lyme disease risk emergence and for development of public health policies on surveillance, prevention and control.

1. Introduction

The black-legged tick, *Ixodes scapularis* Say (1821), is the primary vector of *Borrelia burgdorferi*, the bacterial agent of Lyme disease, in eastern and mid-western United States, where $>23{,}000$ Lyme disease cases occur annually (Bacon et al., 2008). Northward invasive spread of the tick vectors from United States endemic foci Dennis et al. (1998) to non-endemic Canadian habitats is currently a public health concern (Ogden et al., 2009).

Lyme disease risk is changing rapidly in Canada (Leighton et al., 2012). A decade ago *I. scapularis* populations were geographically restricted to specific locations on the north shores of Lake Erie and Lake Ontario, one location in southeast Manitoba and one location in Nova Scotia (Ogden et al., 2005). However, more recently *I. scapularis* tick populations have been identified in multiple locations in southern Manitoba, New Brunswick and Nova Scotia and is spreading widely in some areas of southern Ontario and Quebec (Leighton et al., 2012). In addition, "adventitious" ticks can be found over a wide geographic range of

* Corresponding author. Tel.: +1 450 773 8521.
E-mail address: nicholas.ogden@phac-aspc.gc.ca (N.H. Ogden).

0022-5193/$ - see front matter © 2012 Elsevier Ltd. All rights reserved.
http://dx.doi.org/10.1016/j.jtbi.2012.11.014

Canada (Ogden et al., 2006). These are ticks that are dispersed from reproducing tick populations by hosts (particularly migratory birds: Klich et al., 1996; Morshed et al., 1999; Ogden et al., 2008a). Where climate conditions, host densities and habitat are suitable for establishment these adventitious ticks may seed new, reproducing and self-sustaining tick populations (Ogden et al., 2008c). The conditions under which tick populations can persist may be summarized by the basic reproduction number $\mathcal{R}_0$, a key value in the field of infectious disease epidemiology for assessing the conditions under which micro-or macro-parasites can persist in nature. For microparasites it is defined as the average number of secondary cases produced by one infectious primary case in a totally susceptible population and for macroparasites it is defined as the number of new female parasites produced by a female parasite when there are no density dependent constraints acting anywhere in the life cycle of the parasites (Anderson and May, 1991).

Analysis of a simulation population model of *I. scapularis* (Ogden et al., 2005, 2006, 2008a) suggested that temperature conditions were limiting the establishment of *I. scapularis* in Canada, but that climate change (IPCC, 2001) will permit or accelerate the spread of the tick and Lyme disease risk in Canada, as may be expected for other species (Githeko et al., 2000; Parmesan and Yohe, 2003). Climate affects the survival of tick populations in several ways. First, climate indirectly affects tick survival in being a determinant of the occurrence of suitable communities of vertebrate animal hosts of the ticks, and of vegetation that allows development of a duff layer that provides refuge for off-host ticks from desiccation, drowning and extremes of temperature that can directly kill ticks. Second, host-seeking activity is affected by ambient temperature and humidity. Third, rates of development of ticks from one life stage to the next depend in most cases on temperature, being faster at higher temperature and zero at 0 °C. These factors are reviewed by Ogden et al. (2005) in which they were incorporated into a mechanistic simulation model. Field observations indicate that many woodland habitats in Canada are suitable for survival of ticks off-host, and in such habitats mortality rates of ticks over winter and summer are comparable (Lindsay, 1995; Ogden et al., 2006), most likely because the duff layer insulates ticks from deep freezing in winter and desiccation in the summer.

Ogden et al. (2005) used multiple simulations of their model (Ogden et al., 2005), one for each of a number of locations in southeastern Canada, to obtain a threshold of monthly temperature conditions for *I. scapularis* population survival below which the duration of the lifecycle was too long to support long-term survival for particular field-observed rates of daily per capita mortality of the ticks. This allowed mapping of the geographic extent of limits for *I. scapularis* establishment, development of projected future limits for establishment according to predicted future climate change, as well as risk maps for tick establishment accounting for tick dispersion trajectories (Ogden et al., 2005, 2006, 2008b). These practical and validated outcomes were possible because the simulation model precisely models the effects of temperature (and temperature-independent diapause) as delays in transition from one state to another (e.g. engorged larva to questing nymph) to produce a biologically realistic lifecycle length for the tick given the particular monthly temperature conditions for each location for which a simulation was run. The threshold of temperature condition for tick population survival (i.e. at which the number of ticks is eventually zero) was that at which the lifecycle of the tick is so long that the total number of ticks that die (the sum of daily mortalities) is greater than the number of eggs produced by mated females. This sort of model structure has been used in a number of studies of ticks (Mount and Haile, 1989; Porco, 1999; Dobson et al., 2011) that aim to predict seasons of tick activity and variations in tick abundance in different locations.

This model structure was developed to provide field-comparable values for numbers of ticks as an index of the effective reproductive number at model equilibrium. However, values for $\mathcal{R}_0$ cannot be obtained from this mechanistic model using existing mathematical techniques such as the next generation matrix method. However, we aimed to derive an analytic formula to calculate $\mathcal{R}_0$ so we can evaluate the effects of climate and other environmental changes on $\mathcal{R}_0$. This is desirable because $\mathcal{R}_0$ is the universally accepted value to describe the propensity for a parasite or microparasite to survive and be propagated. To achieve this aim, here we describe a method of conversion of the model into a periodic system of differential equations to which currently developed algorithms for calculating $\mathcal{R}_0$ can be applied directly. We then use the derived $\mathcal{R}_0$ formula for validation of the outcomes of the model, sensitivity analysis and, for the first time, direct estimation of the effects of climate (in terms of ambient temperature) on $\mathcal{R}_0$ of *I. scapularis* to produce a map of $\mathcal{R}_0$ for this tick.

2. Materials and methods

2.1. Tick (I. scapularis) population model and parameterization

To examine the temperature effect on each stage of the tick life cycle, we adapted the tick population model from that of Ogden et al. (2005), which comprises 12 mutually exclusive states of the tick life cycle: egg-lying adult females (x_1), eggs (x_2), hardening larvae (x_3), questing larvae (x_4), feeding larvae (x_5), engorged larvae (x_6), questing nymphs (x_7), feeding nymphs (x_8), engorged nymphs (x_9), questing adults (x_{10}), feeding adult females (x_{11}) and engorged adult females (x_{12}) (Fig. 1). The hosts in the model are a considerable simplification of the community of hosts of *I. scapularis*, but this approach has been found to be adequate in field validation of the previous mechanistic version of the model (e.g. Ogden et al., 2008b). We used the same model framework and many data values from Ogden et al. (2005) however we developed a system that used rates of development and questing activity instead of development durations. This leads to a periodic system of ordinary differential equations rather than a system of delay difference equations. Both types of equations are essentially mathematical simplifications of a complex biological system, but by comparing output from the new model and the original mechanistic model and field observation, we were able to show that the differential equation model developed here adequately describes the biological system for practical purposes and the objectives of our study.

The model comprises 12 equations, one for each model compartment:

$$
\begin{aligned}
x_1' &= d_{12}(t)x_{12} - \mu_1(t)x_1,\\
x_2' &= p(t)f(x_{11})x_1 - (d_2(t)+\mu_2(t))x_2,\\
x_3' &= d_2(t)x_2 - (d_3(t)+\mu_3(t))x_3,\\
x_4' &= d_3(t)x_3 - (d_4(t)+\mu_4(t))x_4,\\
x_5' &= d_4(t)x_4 - (d_5(t)+\mu_5(t,x_5))x_5,\\
x_6' &= d_5(t)x_5 - (d_6(t)+\mu_6(t))x_6,\\
x_7' &= d_6(t)x_6 - (d_7(t)+\mu_7(t))x_7,\\
x_8' &= d_7(t)x_7 - (d_8(t)+\mu_8(t,x_8))x_8,\\
x_9' &= d_8(t)x_8 - (d_9(t)+\mu_9(t))x_9,\\
x_{10}' &= d_9(t)x_9 - (d_{10}(t)+\mu_{10}(t))x_{10},\\
x_{11}' &= \tfrac{1}{2}d_{10}(t)x_{10} - (d_{11}(t)+\mu_{11}(t,x_{11}))x_{11},\\
x_{12}' &= d_{11}(t)x_{11} - (d_{12}(t)+\mu_{12}(t))x_{12}.
\end{aligned}
\tag{1}
$$

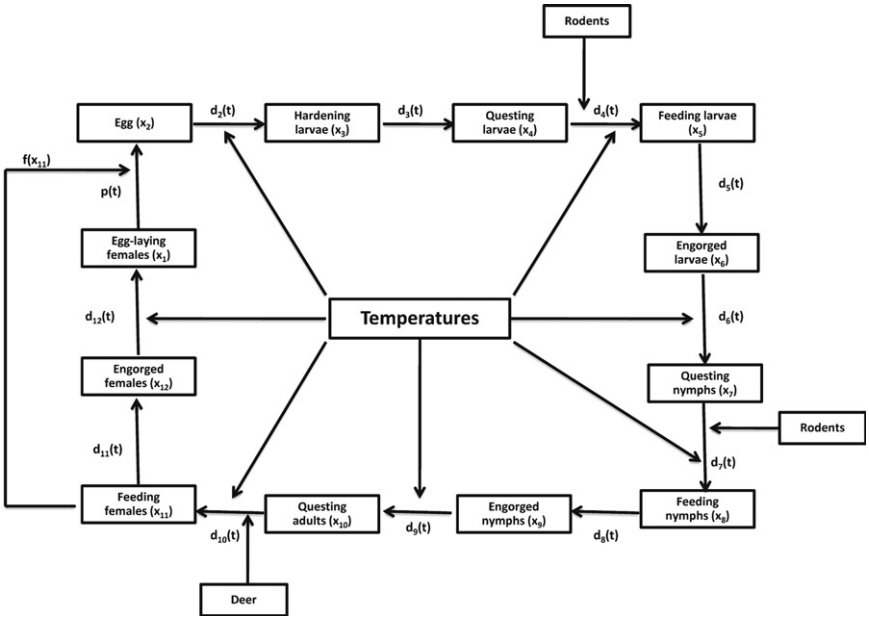

Fig. 1. A diagram of the *I. scapularis* population model adapted from Ogden et al. (2005).

Table 1
Model parameter definitions.

Parameter	Description	Value	Resource
$\mu_1(t)$	Per capita mortality rate of egg-laying adult females	1	O
$\mu_2(t)$	Per capita mortality rate of eggs	0.002	O
$\mu_3(t)$	Per capita mortality rate of hardening larvae	0.006	O
$\mu_4(t)$	Per capita mortality rate of questing larvae	0.006	O
$\mu_5(t,x_5)$	Per capita mortality rate of feeding larvae on rodents	$(0.65+[0.049Ln(\{1.01+x_5\}/R)])$	O
$\mu_6(t)$	Per capita mortality rate of engorged larvae	0.003	O
$\mu_7(t)$	Per capita mortality rate of questing nymphs	0.006	O
$\mu_8(t,x_8)$	Per capita mortality rate of feeding nymphs on rodents	$(0.55+[0.049Ln(\{1.01+x_8\}/R)])$	O
$\mu_9(t)$	Per capita mortality rate of engorged nymphs	0.002	O
$\mu_{10}(t)$	Per capita mortality rate of questing adults	0.006	O
$\mu_{11}(t,x_{11})$	Per capita mortality rate of feeding adults on deer	$(0.5+[0.049Ln(\{1.01+x_{11}\}/D)])$	O
$\mu_{12}(t)$	Per capita mortality rate of engorged adult females	0.0001	O
$p(t)$	Per capita egg production by egg-laying adult females	3000	O
$f(x_{11})$	Reduction in fecundity of egg-laying adult females	$1-[0.01+0.04Ln\{1.01+x_{11}/D\}]$	O
$d_2(t)$	Development rate from eggs to hardening larvae	See text	E
$d_3(t)$	Development rate from hardening larvae to questing larvae	1/21	O
$d_4(t)$	Host attaching rate for questing larvae	See text	E
$d_5(t)$	Development rate from feeding larvae to engorged larvae	1/3	O
$d_6(t)$	Development rate from engorged larvae to questing nymphs	See text	E
$d_7(t)$	Host attaching rate for questing nymphs	See text	E
$d_8(t)$	Development rate from feeding nymphs to engorged nymphs	1/5	O
$d_9(t)$	Development rate from engorged nymphs to questing adults	See text	E
$d_{10}(t)$	Host attaching rate for questing adults	See text	E
$d_{11}(t)$	Development rate from feeding adult females to engorged females	1/10	O
$d_{12}(t)$	Development rate from engorged females to egg-laying females	See text	E
R	Number of rodents	200	O
D	Number of deer	20	O

O: Reference Ogden et al. (2005); E: Estimated (see the main text for detailed discussions how they are estimated). All rates are per day unless otherwise stated.

Here, $x_i' = (d/dt)x_i(t)$ is the derivative of $x_i(t)$ with respect to the time variable t.

The parameters and their values are summarized in Table 1 but the key parameters include:

(1) the progression rate $d_i(t)$ from the i-th stage to the next stage;
(2) the per-capita daily mortality rate $\mu_i(t)$ for stage i;
(3) the per-capita daily egg reproduction rate $p(t)$ by egg-laying females;
(4) rates of density-dependent mortality for each feeding stage of the tick $\mu_5(t,x_5)$, $\mu_8(t,x_8)$, $\mu_{11}(t,x_{11})$;
(5) density-dependent (i.e. associated with the density of ticks feeding on adult tick hosts, which are deer) reduction $f(x_{11})$ in fecundity of egg laying females: $f(x_{11})$ is a decreasing function of x_{11}.

All parameter values were as for the model of Ogden et al. (2005), i.e. they were derived from laboratory and field studies in the Lyme-endemic woodlands of Long Point, Ontario, by Lindsay and collaborators (Lindsay, 1995; Lindsay et al., 1998). The host population was fixed at 200 rodents and 20 deer as in Ogden et al. (2005).

Daily host-finding probabilities varied with host abundance according to the recommendations of Mount et al. (1997) and as calibrated in Ogden et al. (2005) as follows:

λ_{ql}, the host-finding probability for questing larvae $0.0013R^{0.515}$;
λ_{qn}, the host-finding probability for questing nymphs $(0.0013R^{0.515})$; and
λ_{qa}, the host-finding probability for questing adults $0.086D^{0.515}$),

where R is the number of rodents and D is the number of deer.

We assumed that each coefficient is a periodic function of time (t) with the same period of one year.

2.2. Estimation of the development rates

For the study of Ogden et al. (2005) temperature data from the Port Dover weather station were used, this station being the closest to Long Point Ontario where the field data used in model calibration were collected, and where field studies on tick seasonality allows validation. However, Port Dover weather station has closed, so in this study we used temperature data from the Delhi CDA station (obtained from the Environment Canada website: http://www.climate.weatheroffice.gc.ca which is the currently functioning weather station that is closest to Long Point (latitude: 42°36′N; longitude: 80°05′W), so that we can provide simulations with more recent temperature data (temperature normal for 1971–2000). The distance from the Delhi CDA station to Long point is 28.254 km, obtained by the city distance calculator from the website: http://www.javascripter.net/math/calculators/distancecalculator.htm. Some earlier studies of ticks in the field suggest that as far as air temperatures affecting development are concerned, this spatial resolution is adequate (Ogden et al., 2004).

As described in the literature (Lindsay et al., 1998; Ogden et al., 2004), we assumed that the development rates of pre-oviposition period (POP), pre-eclosion period (PEP) and larva-to-nymph are temperature-dependent and development rates of nymph-to-adult are influenced by both temperature and temperature-independent diapause induced by photoperiodicity. Similarly questing activity was assumed to vary with temperature and as in Ogden et al. (2005) the host finding probabilities were varied according to temperature.

As in Ogden et al. (2005) we used the relationships between temperature and tick stage specific development duration derived from field-validated laboratory observations (Ogden et al., 2004)

$$D_1(T) = 1300 \times T^{-1.42} \text{(time delay for the pre-oviposition period)}, \quad (2)$$

$$D_2(T) = 34\,234 \times T^{-2.27} \text{(time delay for the pre-eclosion period of eggs)}, \quad (3)$$

$$D_3(T) = 101\,181 \times T^{-2.55} \text{(time delay for engorged larva to questing nymph)}, \quad (4)$$

$$D_4(T) = 1596 \times T^{-1.21} \text{(time delay for engorged nymph to questing adult)}, \quad (5)$$

where T is the temperature in Celsius (°C). Nymph-to-adult development rates are only determined by temperature for those nymphs that fed before mid-June; all nymphs that fed after mid-June entered diapause (which is temperature independent and likely daylength-induced Ogden et al., 2004) and molted on the same day of the next year, a day predicted by the temperature-development relationship, for nymphs feeding on December 31st of that year.

A key simplification here, compared to the model of Ogden et al. (2005), was that rather than accumulating daily proportions of development from one stage to another, the proportion of development for a particular day of the year (being the reciprocal of the relationship between duration of development and temperature on that day) became the proportion of ticks in a particular life stage that moved to the next life stage on that day, i.e. this became the coefficient (that varied for each day of the year according to temperature) for the rate of movement from engorged to molted ticks, engorged to egg-laying females and eggs to hatched larvae ($d_{12}(t)$, $d_2(t)$, $d_6(t)$ and $d_9(t)$). For the daily development rate ($d_9(t)$) of nymph-to-adult after the summer solstice, when temperature-independent diapause determines development time, the coefficient was the reciprocal of the estimated length of diapause for each day of the duration of diapause. As in Ogden et al. (2005) development was set at zero for all temperatures of 0 °C and below. While this method is not biologically accurate (no tick of any stage develops to the next stage without undergoing the full process of development lasting weeks to months), this simplification would allow development of a differential equation model, and in our validation we aimed to investigate whether this model was adequate or not.

Observations against field data (Ogden et al., 2005) suggested that this method did not produce realistic seasonality of nymphal ticks, so a modified method of calculating the daily rate ($d_6(t)$) at which ticks moved from the engorged larva state to the questing nymph state was used as described in the following. To estimate the larvae-to-nymph development rate for a specific day, temperature data points on that day and subsequent days were used. Suppose the temperature for day i is T_i, then the development duration from engorged larvae to molted nymphs under condition of subsequent constant temperature for day i is $D_3(T_i)$, which is calculated by the relationship between development and temperature (formula (4)). Therefore, the development proportion for day i is $1/D_3(T_i)$. Similarly, the development proportion for day $i+1$ is $1/D_3(T_{i+1})$. When the sum of the accumulative proportion for subsequent n days:

$$\sum_{j=i}^{i+n} \frac{1}{D_3(T_j)},$$

equaled unity, we obtained a number n and then $1/n$ was defined as the development rate of larva-to-nymph at the particular day i.

The 1971–2000 temperature normals used are averages of 30 years data and presented as monthly means. While this was adequate for the mechanistic model of Ogden et al. (2005) we smoothed the temperature-driven periodic coefficients for development by Fourier analysis (see appendix) as shown in Fig. 2.

2.3. Basic reproduction number ($\mathcal{R}_0$)

The basic reproduction number $\mathcal{R}_0$ determines the threshold values at which the tick population model exhibits the change of stability of the tick-free state and the change of population dynamics from persistence to extinction (Diekmann and Heesterbeek, 2000; Wang and Zhao, 2008). More precisely, $\mathcal{R}_0 > 1$ implies the instability of the tick-free state and the persistence of ticks, while $\mathcal{R}_0 < 1$ implies the stability of the tick-free state and hence the extinction of the ticks. Hartemink et al. (2008) presented an approach to estimate the $\mathcal{R}_0$ of tick-borne infections by obtaining the dominant eigenvalue of the next generation matrix of their model equations. This technique is applicable to the case where parameters of the system are constant. Here, we used a recently developed general approach (Bacaër and Guernaoui, 2006; Wang and Zhao, 2008) to evaluate $\mathcal{R}_0$ for time periodic systems.

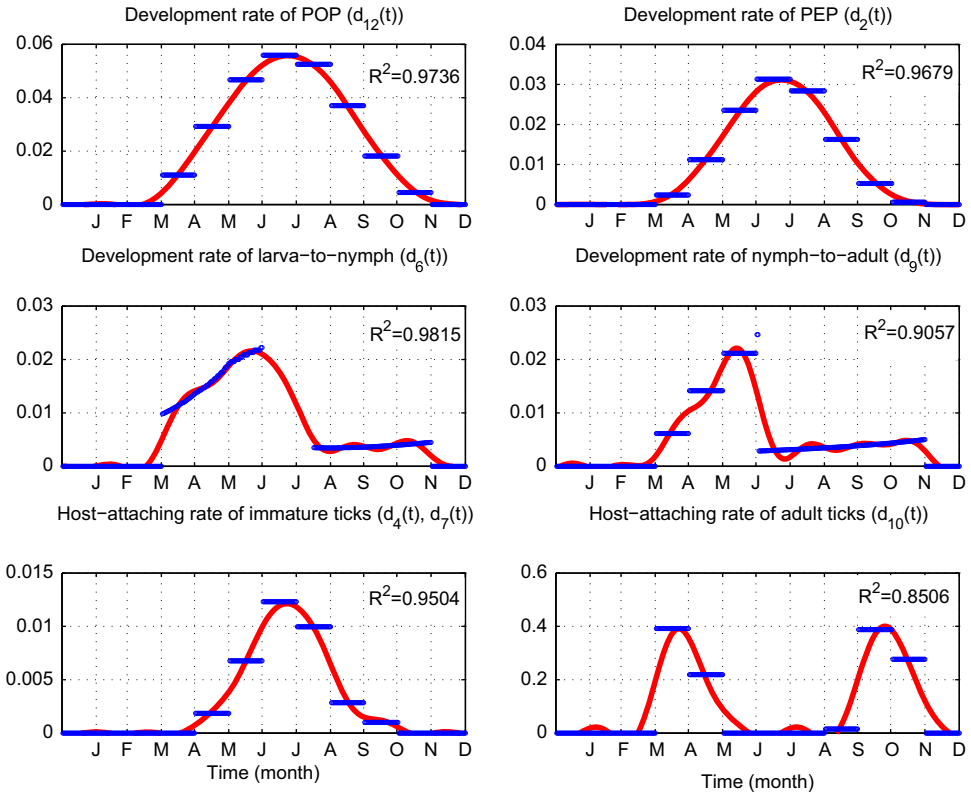

Fig. 2. Development rates and host-attaching rates of *I. scapularis* ticks in a one year period. Blue lines represent development rates or host-attaching rates at each day of the year, calculated from the mean monthly normal temperature data of Delhi CDA for 1971-2000 periods. Red lines represent the development rates and host-attaching rates at each day of the year after smoothing by Fourier series. R^2 are shown. (For interpretation of the references to color in this figure caption, the reader is referred to the web version of this article.)

Table 2
The locations of meteorological stations from which temperature data were used in the simulations. Outcomes of simulations of the current model and that in Ogden et al. (2005) (respectively $\mathcal{R}_0$ and numbers of feeding adult ticks ate equilibrium) are shown.

Station	Location	Mean $DD>0$ °C	Resident tick (Y/N)	Maximum no. of FA at equilibrium	$\mathcal{R}_0$
Ontario					
Point Pelee	41°57′N, 82°31′W	3791	Y	383	3.19
Chatham WCPC	42°23′N, 82°12′W	3911	N	409	3.65
New Glasgow	42°31′N, 81°38′W	3536	N	205	2.06
Port Stanley	42°40′N, 81°13′W	3315	N	104	1.50
Courtright	42°45′N, 82°27′W	3734	N	358	3.04
Delhi CDA	42°52′N, 80°33′W	3441	N	NA	2.04
London Airport	43°02′N, 81°09′W	3355	N	104	1.73
Exeter	43°21′N, 81°29′W	3336	N	100	1.71
Blyth	43°43′N, 81°23′W	3221	N	54	1.30
Hanover	44°07′N, 81°00′W	3100	N	23	1.01
Wiarton Airport	44°45′N, 81°06′W	2959	N	0	0.71
South Baymouth	45°35′N, 82°01′W	2733	N	0	0.52
Timmins Airport	48°34′N, 81°23′W	2351	N	0	0.20
Cochrane	49°04′N, 81°02′W	2256	N	0	0.17
Kapuskasing CDA	49°24′N, 82°26′W	2317	N	0	0.19
Smoky Falls	50°04′N, 82°10′W	2283	N	0	0.19
Quebec					
Hemmingford	45°04′N, 73°43′W	3076	N	87	1.61
St Anicet	45°08′N, 74°21′W	3167	N	126	1.86
Iberville	45°20′N, 73°15′W	3131	N	117	1.80
Montreal McGill	45°30′N, 73°35′W	3409	N	288	2.84
Ste Thérèse Ouest	45°39′N, 73°53′W	3000	N	70	1.50
St Janvier	45°44′N, 73°53′W	2860	N	24	1.19
Fleury	45°48′N, 73°00′W	2969	N	54	1.37
Sorel	46°02′N, 73°07′W	3095	N	129	1.94
St Côme	46°17′N, 73°45′W	2417	N	0	0.38
St Zenon	46°37′N, 73°52′W	2236	N	0	0.20
St Michel des Saints	46°41′N, 73°55′W	2392	N	0	0.35
Grande Anse	47°06′N, 72°56′W	2575	N	0	0.60
La Dore	48°46′N, 72°43′W	2264	N	0	0.26
Chapais 2	49°47′N, 74°51′W	2001	N	0	0.11

DD: Degree days; FA: Feeding adults; $\mathcal{R}_0$: The basic reproduction number; NA: Not available in Ogden et al. (2005).

In the approach recently developed by Bacaër and Guernaoui (2006), Wang and Zhao (2008) the calculation of $\mathcal{R}_0$ is determined by the system (1) linearized at the tick-free state given below:

$$
\begin{aligned}
x_1' &= d_{12}(t)x_{12} - \mu_1(t)x_1,\\
x_2' &= p(t)f(0)x_1 - (d_2(t)+\mu_2(t))x_2,\\
x_3' &= d_2(t)x_2 - (d_3(t)+\mu_3(t))x_3,\\
x_4' &= d_3(t)x_3 - (d_4(t)+\mu_4(t))x_4,\\
x_5' &= d_4(t)x_4 - (d_5(t)+\mu_5(t,0))x_5,\\
x_6' &= d_5(t)x_5 - (d_6(t)+\mu_6(t))x_6,\\
x_7' &= d_6(t)x_6 - (d_7(t)+\mu_7(t))x_7,\\
x_8' &= d_7(t)x_7 - (d_8(t)+\mu_8(t,0))x_8,\\
x_9' &= d_8(t)x_8 - (d_9(t)+\mu_9(t))x_9,\\
x_{10}' &= d_9(t)x_9 - (d_{10}(t)+\mu_{10}(t))x_{10},\\
x_{11}' &= \tfrac{1}{2}d_{10}(t)x_{10} - (d_{11}(t)+\mu_{11}(t,0))x_{11},\\
x_{12}' &= d_{11}(t)x_{11} - (d_{12}(t)+\mu_{12}(t))x_{12}.
\end{aligned}
\tag{6}
$$

The basic reproduction number describes the net reproduction (birth rate minus death rate) per generation when the tick population is small (near the tick-free state). However, since the tick population is stratified by development stages, the calculation of $\mathcal{R}_0$ requires the separation of the processes of birth, development and death. As such, we first introduce the birth matrix $F(t)=(f_{ij}(t))_{12\times 12}$, where $f_{2,1}(t)=p(t)f(0)$ and $f_{i,j}(t)=0$ if $(i,j)\neq(2,1)$. We also need to introduce the progressive matrix $V(t)=V^-(t)-V^+(t)$, with $V^+(t)$ and $V^-(t):=[V_1^-(t)|V_2^-(t)]$ denoting the input and output to a particular tick stage due to development or natural death. These are given by

$$
V^+(t)=\begin{pmatrix}
0 & 0 & 0 & 0 & 0 & 0 & 0 & 0 & 0 & 0 & 0 & d_{12}(t)\\
0 & 0 & 0 & 0 & 0 & 0 & 0 & 0 & 0 & 0 & 0 & 0\\
0 & d_2(t) & 0 & 0 & 0 & 0 & 0 & 0 & 0 & 0 & 0 & 0\\
0 & 0 & d_3(t) & 0 & 0 & 0 & 0 & 0 & 0 & 0 & 0 & 0\\
0 & 0 & 0 & d_4(t) & 0 & 0 & 0 & 0 & 0 & 0 & 0 & 0\\
0 & 0 & 0 & 0 & d_5(t) & 0 & 0 & 0 & 0 & 0 & 0 & 0\\
0 & 0 & 0 & 0 & 0 & d_6(t) & 0 & 0 & 0 & 0 & 0 & 0\\
0 & 0 & 0 & 0 & 0 & 0 & d_7(t) & 0 & 0 & 0 & 0 & 0\\
0 & 0 & 0 & 0 & 0 & 0 & 0 & d_8(t) & 0 & 0 & 0 & 0\\
0 & 0 & 0 & 0 & 0 & 0 & 0 & 0 & d_9(t) & 0 & 0 & 0\\
0 & 0 & 0 & 0 & 0 & 0 & 0 & 0 & 0 & d_{10}(t) & 0 & 0\\
0 & 0 & 0 & 0 & 0 & 0 & 0 & 0 & 0 & 0 & d_{11}(t) & 0
\end{pmatrix},
$$

$$
V_1^-(t)=\begin{pmatrix}
\mu_1(t) & 0 & 0 & 0 & 0 & 0\\
0 & d_2(t)+\mu_2(t) & 0 & 0 & 0 & 0\\
0 & 0 & d_3(t)+\mu_3(t) & 0 & 0 & 0\\
0 & 0 & 0 & d_4(t)+\mu_4(t) & 0 & 0\\
0 & 0 & 0 & 0 & d_5(t)+\mu_5(t,0) & 0\\
0 & 0 & 0 & 0 & 0 & d_6(t)+\mu_6(t)\\
0 & 0 & 0 & 0 & 0 & 0\\
0 & 0 & 0 & 0 & 0 & 0\\
0 & 0 & 0 & 0 & 0 & 0\\
0 & 0 & 0 & 0 & 0 & 0\\
0 & 0 & 0 & 0 & 0 & 0\\
0 & 0 & 0 & 0 & 0 & 0
\end{pmatrix},
$$

and

$$
V_2^-(t)=\begin{pmatrix}
0 & 0 & 0 & 0 & 0 & 0\\
0 & 0 & 0 & 0 & 0 & 0\\
0 & 0 & 0 & 0 & 0 & 0\\
0 & 0 & 0 & 0 & 0 & 0\\
0 & 0 & 0 & 0 & 0 & 0\\
0 & 0 & 0 & 0 & 0 & 0\\
d_7(t)+\mu_7(t) & 0 & 0 & 0 & 0 & 0\\
0 & d_8(t)+\mu_8(t,0) & 0 & 0 & 0 & 0\\
0 & 0 & d_9(t)+\mu_9(t) & 0 & 0 & 0\\
0 & 0 & 0 & d_{10}(t)+\mu_{10}(t) & 0 & 0\\
0 & 0 & 0 & 0 & d_{11}(t)+\mu_{11}(t,0) & 0\\
0 & 0 & 0 & 0 & 0 & d_{12}(t)+\mu_{12}(t)
\end{pmatrix}.
$$

In the above progressive matrices, $V_{i,j}^+(t)$ is the input (development) rate of the ticks from the x_j-stage to the x_i-stage, and $V_{i,j}^-(t)$ is the output rate at which ticks at the x_j-stage move out to the x_i-stage, or die.

With these matrix notations, we can rewrite the linear system (6) as

$$
\frac{dx(t)}{dt}=(F(t)-V(t))x(t).
$$

Whether the tick population grows or decays over time is determined by how the population is (dynamically) transferred from the beginning to the end of a year. The growth or decay rate of the tick population is determined by the transfer rate. To calculate this transfer rate, we need to study the so-called fundamental matrix solution of the above linear periodic system. These are the solutions of the linear system with special initial conditions (see Hale, 1980) so that all other solutions with arbitrarily given initial condition can be expressed analytically in terms of the fundamental matrix solution and the initial condition. The work in Bacaër and Guernaoui (2006) and Wang and Zhao (2008) develops a general approach that ties the fundamental matrix solution of the above linear system and the growth or decay rate of tick population to the evolution operator $Y(t,s)$, $t\geq s$, of the linear periodic system $y'=-V(t)y$. This operator is defined as follows: for each $s\in\mathbb{R}$, the 12×12 matrix $Y(t,s)$ satisfies

$$
\frac{d}{dt}Y(t,s)=-V(t)Y(t,s)\quad \forall t\geq s,\quad Y(s,s)=I,
$$

where I is the 12×12 identity matrix. To relate to the basic reproduction number, we let C_T denote the collection of all possible initial tick populations distributed over the period $[0,T]$-the set of all continuous periodic functions from $[0,T]$ to R^{12} equipped with certain mathematical structures such as the super-norm . For a fixed initial tick population distribution $\phi\in C_T$, $F(s)\phi(s)$ is the rate of new ticks produced by the initial ticks who were introduced at time s, and $Y(t,s)F(s)\phi(s)$ represents the distribution of those ticks who were newly produced at time s and remained alive at time t for $t\geq s$. Hence

$$
\psi(t)=\int_{-\infty}^{t}Y(t,s)F(s)\phi(s)\,ds=\int_0^{\infty}Y(t,t-a)F(t-a)\phi(t-a)\,da
$$

is the distribution of accumulated ticks at time t produced by all those ticks $\phi(s)$ introduced at the previous time. This naturally leads to the linear operator $L:C_T\to C_T$ given by

$$
(L\phi)(t)=\int_0^{\infty}Y(t,t-a)F(t-a)\phi(t-a)\,da\ \forall t\in\mathbb{R},\ \phi\in C_T.
$$

It then follows from Wang and Zhao (2008) that L is the next generation operator, and the basic reproduction number is $\mathcal{R}_0:=\rho(L)$, the spectral radius of L.

2.4. Sensitivity analysis

To assess the sensitivity of model outcomes to variations in each parameter we carried out a global sensitivity analysis with the Monte Carlo-based Latin Hypercube Sampling (LHS) variance method (Mckay et al., 1979; Marino et al., 2008) using the $\mathcal{R}_0$ as the outcome variable. All the parameters in the investigation are changed by 20% from their start values and then 600 simulations were run. Sensitivity to each given parameter was measured by the partial rank correlation coefficient (PRCC) between the parameter and the outcome variable ($\mathcal{R}_0$).

2.5. Simulation and validation

We performed model simulations using temperature data (mean monthly temperature normal data for the period 1971–2000) from 16 meteorological stations in southern Ontario and 14 meteorological stations in Quebec. In each case $\mathcal{R}_0$ was calculated and these were compared with the data obtained in simulations of the model of Ogden et al. (2005). From these latter data, Ogden et al. (2005) produced a graph of the relationship between the cumulative degree days above 0 °C for each meteorological station and an index of the numbers of ticks at model equilibrium. By finding the *x*-axis intercept of the fitted regression line the temperature conditions at which the number of ticks was zero in the model were determined. This graph was reproduced and compared with the $\mathcal{R}_0$ values obtained for the same locations using simulations of the model developed here.We also compared the seasonality of tick activity produced by the new model and the model in Ogden et al. (2005).

2.6. Mapping

A map of $\mathcal{R}_0$ values >1 in Canada east of the Rocky Mountains (a different tick species transmits Lyme west of these) was prepared using the relationship between $\mathcal{R}_0$ and temperature conditions (using cumulative annual degree-days >0 °C [$DD>0$ °C] as an index) estimated from the simulations for meteorological stations in Quebec (which provides a more cautious assessment of risk of *I. scapularis* invasion-see results section) as described above. The method used was similar to that described in Ogden et al. (2008b): $DD>0$ °C values were obtained for 2368 meteorological stations that had data for >15 years during the period 1971–2000 and these values were converted to $\mathcal{R}_0$ values according to the relationship described above, and then $\mathcal{R}_0$ values were interpolated by inverse distance weighting across a 4×4 km pixelated landscape with pixel size 4×4 km.

3. Results

3.1. Model simulations

There was considerable concurrence in the outcomes of simulations by the modified model and the model of Ogden et al. (2005). $\mathcal{R}_0$ for *I. scapularis* at Long Point, Point Pelee and Chatham, sites where *I. scapularis* populations were known to be established during the period 1971–2000, was estimated at 1.5, 3.19 and 3.65, respectively (Table 2). The temperature conditions identified by the two models as being those at which $\mathcal{R}_0=1$ (i.e. threshold conditions for tick population persistence) were effectively identical at 3100 $DD>0$ °C (Fig. 3). The relationship between $\mathcal{R}_0$ and $DD>0$ °C was essentially linear and, as in Ogden et al. (2005) slightly different for Ontario and Quebec ($\mathcal{R}_0=0.0033DD>0\,^{\circ}\mathrm{C}-9.358$ and $\mathcal{R}_0=0.003DD>0\,^{\circ}\mathrm{C}-7.551$, respectively). Based on the aforementioned relationship between $\mathcal{R}_0$ and temperature conditions estimated from the simulations for meteorological stations, an $\mathcal{R}_0$ map for Canada was developed (Fig. 4). Simulated seasonality of ticks by the two models were also similar (Fig. 6).

3.2. Sensitivity analysis

Fig. 5 presents the Partial Rank Correlation Coefficients (PRCC) for each parameter used in the sensitivity analysis that, in turn, explains the sensitivity of the $\mathcal{R}_0$ value to each parameter. The model was particularly sensitive (absolute PRCC >0.7) to changes in summer (July, August, June) mean temperatures and host abundance of immature ticks. $\mathcal{R}_0$ was moderately sensitive to development rates of feeding ticks and mortalities of immature questing ticks. $\mathcal{R}_0$ was particularly insensitive to mean temperatures in April/October/November, mortalities of engorged/questing adults, mortalities of hardening larvae, number of deer (absolute PRCC <0.2). Table 3 lists parameters in a descending order of importance.

4. Discussion

Our study applies a new mathematical approach to predict the survival and occurrence of the tick vector of Lyme disease, and by inference the spread of Lyme disease risk, using a direct $\mathcal{R}_0$-based approach.

Models of vectors and vector-borne diseases (including ticks and tick-borne pathogens) include those that aim to explore theoretically the behaviors of the systems, which may or may not use $\mathcal{R}_0$ as an index of the relative contributions or effects of different model parameters (e.g. Norman et al., 1999; Schmidt and Ostfeld, 2001; Rosá et al., 2003; Rosá and Pugliese, 2007; Randolph et al., 1999; Caraco et al., 2002; Ghosh and Pugliese, 2004; Foppa, 2005; Hartemink et al., 2008); and simulation models that aim to explicitly simulate aspects of the biology of vectors and vector-borne disease systems as accurately as possible (e.g. Mount and Haile, 1989; Mount et al., 1997; Porco, 1999; Ogden et al., 2005; Dobson et al., 2011). The outcomes of the latter models have been used to produce predictive and risk assessment tools for practical animal health and public health decision-making . Examples include risk maps for Lyme disease, Bluetonge virus and Leishmaniasis (e.g. Hartemink et al., 2008, 2009, 2011), but none to date have been able to produce maps using a dynamical version of $\mathcal{R}_0$.

Here we have developed a relatively highly parameterized model that employs the next generation matrix approach to obtain values for $\mathcal{R}_0$ in complex systems with multiple differential Dobson (2004); Hartemink et al. (2008, 2011) and Hartemink et al. (2008, 2011). Special attention had to be made to ensure that the simplification of the mechanistic model of Ogden et al. (2005) allowed retention of a key feature-a realistic modeling of the effect of temperature on total tick mortality indirectly induced by variations in the length of the tick lifecycle.

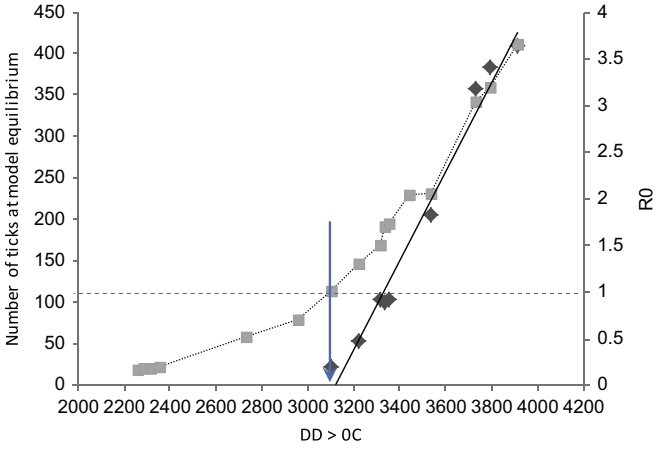

Fig. 3. $\mathcal{R}_0$ calculated in this study (light gray squares), as well as the maximum numbers of feeding adult ticks at equilibrium using the model of Ogden et al. (2005) (dark gray lozenges with linear trend line), are plotted against the mean annual number of degree-days >0 °C ($DD>0$ °C) for the meteorological stations in Ontario that provided temperature data for the simulations. The horizontal dashed line indicate $\mathcal{R}_0=1$ on the secondary axis and the arrow indicates the value of $DD>0$ °C at which $\mathcal{R}_0$ was estimated at 1 by both models.

Both models produce near identical results in terms of identifying the temperature conditions at which $\mathcal{R}_0$ falls below unity, i.e. they identify threshold environmental conditions for survival of the tick *I. scapularis*, which is a prerequisite for Lyme disease risk emergence. However using the model developed here we can obtain and map direct estimates for $\mathcal{R}_0$ for *I. scapularis*. As a consequence we could produce an $\mathcal{R}_0$ map for *I. scapularis* for regions of Canada east of the Rocky Mountains (although this assumes habitat in terms of host community and off-host tick survival is constant). The geographic extent of territory where $\mathcal{R}_0 > 1$ is similar to that for the map generated by the model of Ogden et al. (2005) although the $\mathcal{R}_0$ map immediately provides a gradient of suitability above $\mathcal{R}_0 = 1$. To our knowledge this is the first $\mathcal{R}_0$ map for an arthropod tick vector.

Sensitivity analysis produced expected results. Because *I. scapularis* is an obligate parasite, host densities have a strong effect on tick abundance although deer abundance must fall below a certain threshold before the abundance of ticks falls significantly (Ogden et al., 2007). Also, variations in temperature conditions during the warmer months have a greater effect on $\mathcal{R}_0$ than changes during the coolest months because of the non-linear relationship between temperature and tick development rates (Ogden et al., 2004). This is also the reason why the relationships between $\mathcal{R}_0$ and $DD > 0$ °C are slightly different for simulations in southern Quebec and southern Ontario: summers are shorter but warmer in southern Quebec and $\mathcal{R}_0$ is rather higher than in southern Ontario for locations having the same $DD > 0$ °C values.

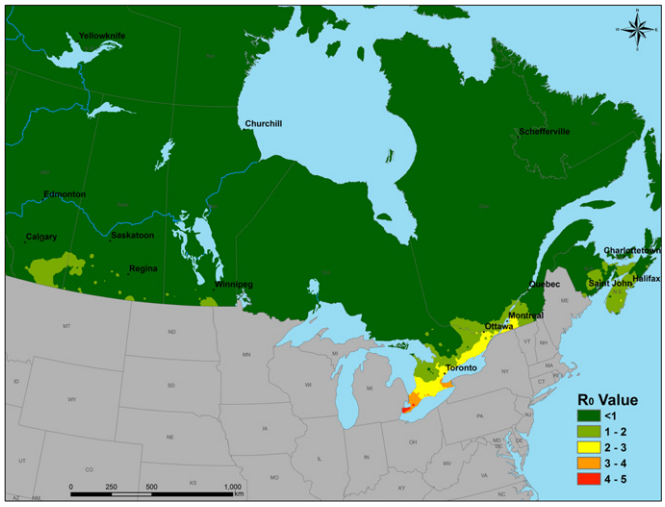

Fig. 4. A map of $\mathcal{R}_0$ values for *I. scapularis* for Canada east of the Rocky Mountains assuming that all model parameter values other than those affected by temperature conditions are the same as those used in model simulations in this paper.

The accuracy of the model developed here was demonstrated by the model's ability to identify a threshold temperature condition for tick population persistence of 3100 $DD > 0$ °C, which was the same as that identified by the model of Ogden et al. (2005). This value has been extensively validated in the field against the locations of confirmed endemic populations of *I. scapularis* (Ogden et al., 2008b). The appropriateness of our approach was also demonstrated by the ability of the model to simulate tick seasonality expected in northeastern North America (Ogden et al., 2005). The model was also, however, able to quantify relationships between temperature and $\mathcal{R}_0$. When $DD > 0$ °C was greater than the threshold condition for $\mathcal{R}_0 = 1$, $\mathcal{R}_0$ increased by approximately 0.5 for every 100 increase in $DD > 0$ °C (see Fig. 3) although this will vary with a number of model parameters such as host finding rates and host densities (Ogden et al., 2005). Subsequent empirical and field-observation studies have underlined the importance of temperature as a driver of establishment of *I. scapularis* (Ogden et al., 2010; Leighton et al., 2012), and future studies must aim to precisely model effects of climate change on $\mathcal{R}_0$ for *I. scapularis*. Nevertheless, we have developed here a methodology for estimating $\mathcal{R}_0$ for ticks that can be used for practical animal and public health purposes.

The model presented here was parameterized in mostly the same way, and with the same values, as the model in Ogden et al. (2005), and the impact of variation in these on tick survival and abundance were explored in that paper as well as here. The factors affecting the threshold temperature conditions for $\mathcal{R}_0 \geq 1$ are (and were) the relationship between temperature and development rates, and the per-capita daily mortality rates of free-living ticks (Ogden et al., 2005). As mentioned in Ogden et al. (2005) variations in the former could occur with different genotypes of *I. scapularis* although we have no evidence for that.

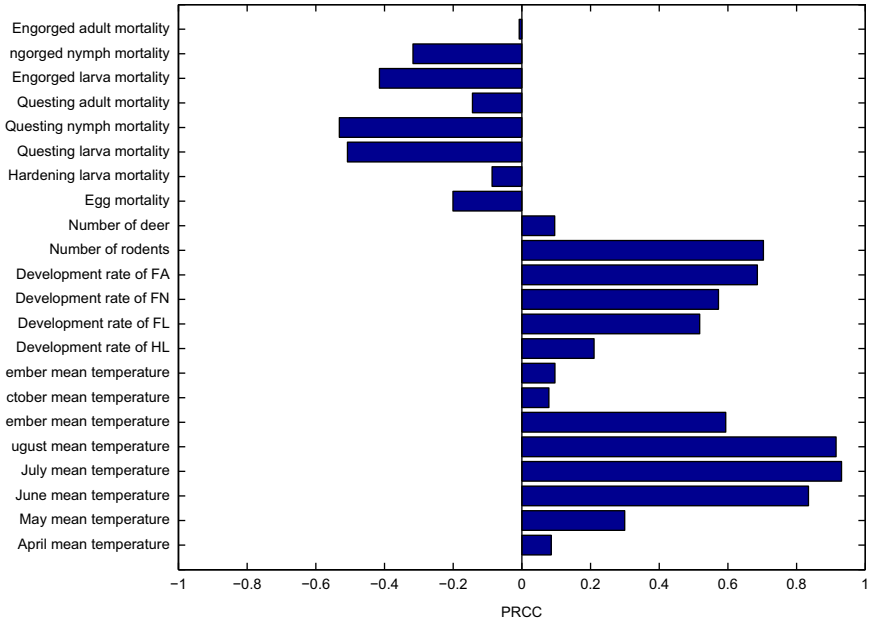

Fig. 5. Global sensitivity analysis of $\mathcal{R}_0$ to a 20% change in the value of the parameters over 600 simulations. PRCC: Partial rank correlation coefficient.

Table 3
PRCC results for each parameter in the LHS/PRCC sensitivity analysis.

Parameter description	PRCC	p-Value	Significant ($p < 0.01$)
July mean monthly temperature	0.93103	8.9284e−255	*
August mean monthly temperature	0.91524	5.8975e−230	*
June mean monthly temperature	0.83477	1.1508e−151	*
Number of rodents (R)	0.70357	1.1792e−087	*
Development rate of feeding adults (d_{11})	0.68585	1.1092e−081	*
September mean monthly temperature	0.5938	1.861e−056	*
Development rate of feeding nymphs (d_8)	0.57262	9.5196e−052	*
Questing nymph mortality (μ_7)	−0.53144	1.6233e−043	*
Development rate of feeding larvae (d_5)	0.51807	4.4421e−041	*
Questing larva mortality (μ_4)	−0.50762	3.0201e−039	*
Engorged larva mortality (μ_6)	−0.41474	1.7793e−025	*
Engorged nymph mortality (μ_9)	−0.31698	5.5725e−015	*
May mean monthly temperature	0.29966	1.7717e−13	*
Development rate of hardening larvae (d_3)	0.21037	3.2498e−007	*
Egg mortality (μ_2)	−0.20051	1.1513e−006	*
Questing adult mortality (μ_{10})	−0.14358	0.00052924	*
November mean monthly temperature	0.096436	0.020294	
Number of deer (D)	0.09592	0.020977	
Hardening larva mortality (μ_3)	−0.086626	0.037175	
April mean monthly temperature	0.08569	0.039279	
October mean monthly temperature	0.078827	0.058012	
Engorged adult mortality (μ_{12})	−0.0076705	0.85388	

This table summarizes results in terms of PRCC and p-value when changing model parameter values by 20% from their start values. The start values of mean monthly temperature are adapted from Delhi CDA weather station over 1971–2000 period, and all other parameters are the same as those in Table 1 in this study. The sign of PRCC represents the positive (+) or negative (−) response of $\mathcal{R}_0$ to the changed parameter values. The parameters are listed in descending order of the magnitude of the sensitivity of $\mathcal{R}_0$ to changes in their values. *: Significant at the $p < 0.01$.

Variations in the latter could occur due to the characteristics of the habitats in which the ticks live, so for some locations the map in Fig. 4 may rather over or under estimate risk (see Ogden et al., 2006a for details). Above the threshold conditions for $\mathcal{R}_0 \geq 1$, the magnitude of the relationship between $\mathcal{R}_0$ and $DD > 0$ °C (and the abundance of ticks at equilibrium in Ogden et al., 2005) depend on parameters such as host finding rates and host densities and these will vary from one location to the next according to different ecological conditions, but these factors will vary at a scale that is too fine for visualization at a national scale. They may well be very significant at a local, operational scale, however. Stochastic effects are not included in the model because of lack of information on which to parameterize them. Therefore, the model in this paper estimates the main macroclimatic influence on possible tick population occurrence in Canada upon which more local variations in ecological conditions will be superimposed to determine $\mathcal{R}_0$ at these more precise locations. It would be expected that at marginal temperature conditions, stochastic events could drive recently established populations to extinction, but ticks are constantly re-introduced by migratory birds and other hosts to re-establish populations (Ogden et al., 2008a, 2008b) so stochastic fade out of tick populations would likely be only temporary in southern Canada. Furthermore, tick populations are resilient to wide temperature and humidity variations on a short (day-to-year) time scale because ticks actively seek effective refugia from climatic extremes in the surface layers of the forest floor, and there is latency in changes in development rates in response to fluctuations in temperatures (Ogden et al., 2004).

The methodology developed here can be expanded to directly model the effects on $\mathcal{R}_0$ for the agent of Lyme disease, *Borrelia burgdorferi*, of a greater range of environmental factors that determine Lyme disease risk establishment such as host densities, community structure, habitat effects on tick mortality, and immigration rates for ticks and *B. burgdorferi*. It could also be adapted for other tick species in other parts of the world.

5. Conclusion

We have developed a methodology for modelling the biology of the tick vector of Lyme disease to produce a value for $\mathcal{R}_0$ according to ambient temperature conditions. It can also be adapted to investigate how $\mathcal{R}_0$ may vary with other environmental variables such as host densities and habitat effects on tick mortality. The model can be used directly to assess the risk from emerging Lyme disease in Canada (and elsewhere) that will allow more effective planning of public health policy, and development/evaluation of preventive and control strategies. While the precise parameterizations of the model is relevant for Canada and the northeastern USA, the methodology is applicable to other tick species elsewhere in the world. This tool is particularly powerful by providing a value for $\mathcal{R}_0$, which is the universally accepted value translatable to all branches of epidemiology including those involved in vector borne diseases (The malERA Consultative Group on Modeling The malERA Consultative Group on Modeling, 2011) and emerging infectious diseases (e.g. Webb et al., 2004; Gumel et al., 2004; Ferguson et al., 2005; Smith et al., 2007; Fraser et al., 2009). In the process we have produced estimates of $\mathcal{R}_0$ for locations in Canada where *I. scapularis* are established, and produced the first $\mathcal{R}_0$ map for an arthropod vector.

Acknowledgments

This work has been partially supported by the Canada Research Chairs Program, Natural Sciences and Engineering Research Council of Canada, MITACS, GEOIDE, the Centre for Disease Modelling, and Public Health Agency of Canada. We are grateful to three anonymous referees for their careful reading and valuable comments which led to improvements of our manuscript.

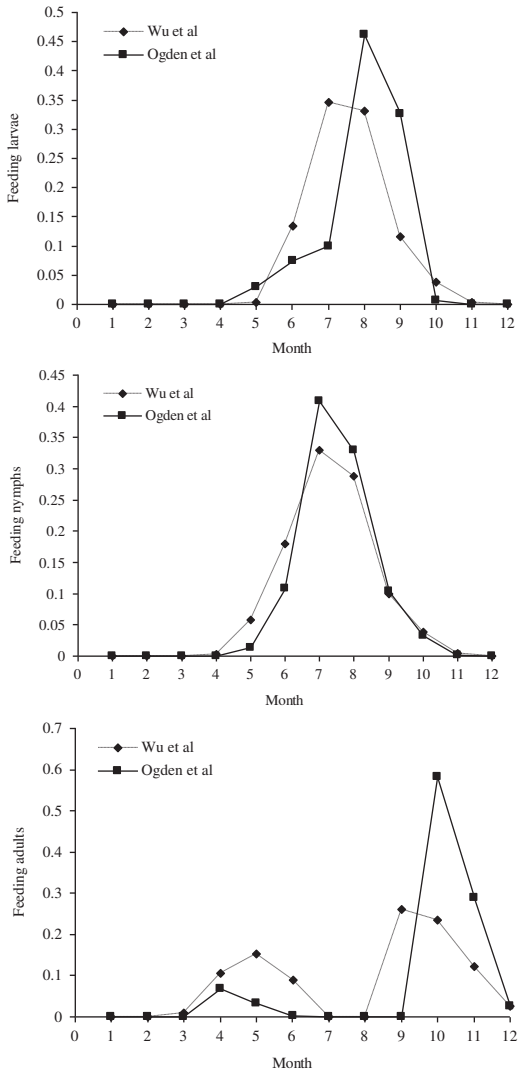

Fig. 6. Comparison of model simulations of the seasonality of ticks (lozenges) generated by our model using mean monthly temperatures from Delhi CDA, Ontario meteorological station, and the seasonality simulated in Ogden et al. (2005) (square). The number of y-axis is the proportion of ticks of that instar feeding on the same day as field observations, against presented as a proportion of the total annual number of ticks feeding on the same dates in the simulation.

Appendix A. Fourier series analysis

In our model, there are seven periodic coefficients to be determined for the given meteorological stations for the 1971–2000 period: $d_{12}(t)$, $d_2(t)$, $d_6(t)$, $d_9(t)$ (development rates of POP, PEP, larva-to-nymph and nymph-to-adult, respectively) and $d_4(t)$, $d_7(t)$ and $d_{10}(t)$ (host attaching rates of larvae, nymphs and adults, respectively). The host attaching rates are given by the following relationship

$$d_4(t)=\lambda_{ql}\times\theta^i(t),\quad d_7(t)=\lambda_{qn}\times\theta^i(t),\quad d_{10}(t)=\lambda_{qa}\times\theta^a(t),\qquad \text{(A1)}$$

with $\theta^i(t)$, $\theta^a(t)$ being the respective activity proportions of immature and adult ticks which depend on temperature (Fig. A1).

The following "7th order Fourier series" was employed to estimate the seven periodic coefficients of the tick stage and seasonally specific development and activity

$$f(t)=c_0+\sum_{i=1}^{7}\left(a_i\sin\frac{2\pi it}{365}+b_i\cos\frac{2\pi it}{365}\right).\qquad \text{(A2)}$$

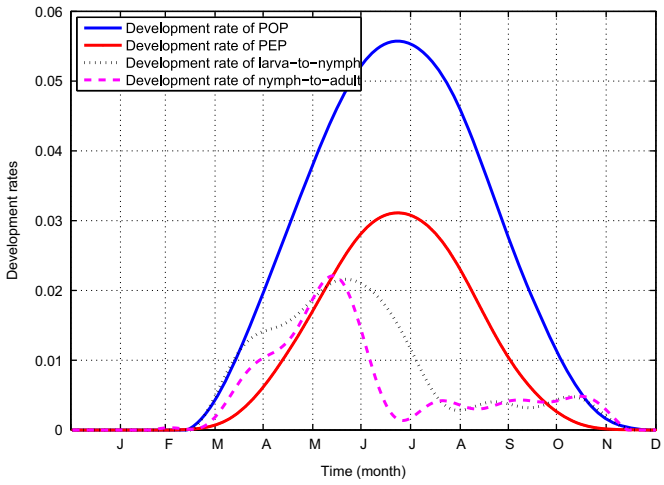

Fig. A1. Fourier series projected development rates of POP ($d_{12}(t)$), PEP ($d_2(t)$), larva-to-nymph ($d_6(t)$) and nymph-to-adult ($d_9(t)$) from the 1971–2000 mean monthly normal temperature at Delhi CDA meteorological station.

MATLAB (R2010a) was used for the Fourier series analysis by fitting the tick data into the Eq. (A2). For instance, Fig. 2 presents the fitted development rates of POP, PEP, larva-to-nymph and nymph-to-adult at Delhi CDA meteorological station for the 1971–2000 periods, the detailed periodic functions are presented in the following subsection.

Appendix B. Periodic functions at Delhi CDA meteorological station for the 1971–2000 periods

In what follows, we used $t(m365)$ to denote the modular after division $(t/365)$. The periodic developmental rate of POP is given by

$$d_{12}(t)=\frac{\text{sign}[(t(m365)-47.8683)(358.9047-t(m365))]+1}{2}\times f_1(t),$$

where

$$f_1(t)=c_0+\sum_{i=1}^{7}\left(a_i\sin\frac{2i\pi t}{365}+b_i\cos\frac{2i\pi t}{365}\right),$$

$c_0=0.02139$, $a_1=-0.01048$, $b_1=-0.02676$, $a_2=0.004188$,
$b_2=0.005002$, $a_3=0.000749$, $b_3=0.00054$, $a_4=0.000213$,
$b_4=-0.000291$, $a_5=-0.000038$, $b_5=-0.000159$, $a_6=-0.000188$,
$b_6=0.000140$, $a_7=-0.000088$, $b_7=0.0000139$;

the periodic developmental rate of PEP is given by

$$d_2(t)=\frac{\text{sign}[(t(m365)-35.8068)(355.5969-t(m365))]+1}{2}\times f_2(t),$$

where

$$f_2(t)=c_0+\sum_{i=1}^{7}\left(a_i\sin\frac{2i\pi t}{365}+b_i\cos\frac{2i\pi t}{365}\right),$$

$c_0=0.009975$, $a_1=-0.005363$, $b_1=-0.01394$, $a_2=0.003866$,
$b_2=0.004296$, $a_3=-0.000659$, $b_3=-0.000245$, $a_4=-0.000099$,
$b_4=-0.000123$, $a_5=0.000031$, $b_5=0.000007$, $a_6=-0.000023$,
$b_6=0.000091$, $a_7=-0.000004$, $b_7=-0.000079$;

the periodic developmental rate of larva-to-nymph is given by

$$d_6(t)=\frac{\text{sign}[(t(m365)-53.3081)(351.8854-t(m365))]+1}{2}\times f_3(t),$$

where

$$f_3(t) = c_0 + \sum_{i=1}^{5}\left(a_i \sin\frac{2i\pi t}{365} + b_i \cos\frac{2i\pi t}{365}\right),$$

$c_0 = 0.006907$, $a_1 = 0.001712$, $b_1 = -0.008659$, $a_2 = -0.003768$,
$b_2 = 0.002882$, $a_3 = 0.000717$, $b_3 = -0.00127$, $a_4 = 0.000972$,
$b_4 = 0.00057$, $a_5 = -0.000064$, $b_5 = -0.00115$, $a_6 = -0.000041$,
$b_6 = 0.000036$, $a_7 = 0.000079$, $b_7 = 0.000655$;

the periodic developmental rate of nymph-to-adult is given by

$$d_9(t) = \frac{\text{sign}[(t(m365) - 51.2829)(347.2452 - t(m365))] + 1}{2} \times f_4(t),$$

where

$$f_4(t) = c_0 + \sum_{i=1}^{5}\left(a_i \sin\frac{2i\pi t}{365} + b_i \cos\frac{2i\pi t}{365}\right),$$

$c_0 = 0.005122$, $a_1 = 0.001326$, $b_1 = -0.00574$, $a_2 = -0.004511$,
$b_2 = 0.001516$, $a_3 = 0.002741$, $b_3 = -0.0006858$, $a_4 = -0.001363$,
$b_4 = -0.0003076$, $a_5 = 0.00155$, $b_5 = -0.0004824$, $a_6 = -0.0009726$,
$b_6 = 0.0001277$, $a_7 = 0.001129$, $b_7 = 8.877e{-}005$;

the periodic host attaching rate of immature (larva, nymph) $d_4(t)$ (or $d_7(t)$) is given by

$$d_4(t) = \frac{\text{sign}[(t(m365) - 106.9692)(315.0422 - t(m365))] + 1}{2} \times f_5(t),$$

where

$$f_5(t) = c_0 + \sum_{i=1}^{7}\left(a_i \sin\frac{2i\pi t}{365} + b_i \cos\frac{2i\pi t}{365}\right),$$

$c_0 = 0.002924$, $a_1 = -0.001779$, $b_1 = -0.004538$, $a_2 = 0.001854$,
$b_2 = 0.002125$, $a_3 = -0.001022$, $b_3 = -0.000588$, $a_4 = 0.000431$,
$b_4 = -0.000036$, $a_5 = -0.000065$, $b_5 = 0.000173$, $a_6 = -0.000079$,
$b_6 = 0.000043$, $a_7 = -0.000063$, $b_7 = -0.0001740$;

and the periodic host finding rate of adults is given by

$$d_{10}(t) = \text{sign}[(t(m365) - 74.2957)(t(m365) - 175.3725)\cdot (t(m365) - 254.2905)(356.5154 - t(m365))] + 1/2 \times f_6(t),$$

where

$$f_6(t) = c_0 + \sum_{i=1}^{7}\left(a_i \sin\frac{2i\pi t}{365} + b_i \cos\frac{2i\pi t}{365}\right),$$

$c_0 = 0.1077$, $a_1 = -0.008856$, $b_1 = 0.007085$, $a_2 = -0.1382$,
$b_2 = -0.1115$, $a_3 = -0.006589$, $b_3 = -0.005471$, $a_4 = 0.09107$,
$b_4 = -0.01059$, $a_5 = 0.006597$, $b_5 = -0.007067$, $a_6 = -0.02838$,
$b_6 = -0.002206$, $a_7 = 0.001399$, $b_7 = 0.005272$.

References

Anderson, R.M., May, R.M., 1991. Infectious Diseases of Humans: Dynamics and Control. Oxford University Press, Oxford.

Bacaër, N., Guernaoui, S., 2006. The epidemic threshold of vector-borne diseases with seasonality: the case of cutaneous leishmaniasis in Chichaoua, Morocco. J. Math. Biol. 53, 421–436, http://dx.doi.org/10.1007/s00285-006-0015-0.

Bacon, R.M., Kugeler, K.J., Mead, P.S., 2008. Surveillance for Lyme disease-United States, 1992–2006. MMWR Surveillance Summ. 57, 1–9.

Caraco, T., Glavanakov, S., Chen, G., Flaherty, J.E., Ohsumi, T.K., Szymanski, B.K., 2002. Stage-structured infection transmission and a spatial epidemic: a model for Lyme disease. Am. Nat. 160, 348–359, http://dx.doi.org/10.1086/341518.

Dennis, D.T., Nekomoto, T.S., Victor, J.C., Paul, W.S., Piesman, J., 1998. Reported distribution of *Ixodes scapularis* and *Ixodes pacificus* (Acari: Ixodidae) in the United States. J. Med. Entomol. 35, 629–638.

Diekmann, O., Heesterbeek, J.A.P., 2000. Mathematical Epidemiology of Infectious Diseases: Model Building, Analysis and Interpretation. Wiley, New York.

Dobson, A., 2004. Population dynamics of pathogens with multiple host species. Am. Nat. 164, S64–78, http://dx.doi.org/10.1086/424681.

Dobson, A.D.M., Finnie, T.J.R., Randolph, S.E., 2011. A modified matrix model to describe the seasonal population ecology of the European tick Ixodes ricinus. J. Appl. Ecol. 48, 1017–1028, http://dx.doi.org/10.1111/j.1365-2664.2011.02003.x.

Ferguson, N.M., Cummings, D.A., Cauchemez, S., Fraser, C., Riley, S., Meeyai, A., Iamsirithaworn, S., Burke, D.S.D.S., 2005. Strategies for containing an emerging influenza pandemic in Southeast Asia. Nature 437, 209–214, http://dx.doi.org/10.1038/nature04017.

Foppa, I.M., 2005. The basic reproductive number of tick-borne encephalitis virus: an empirical approach. J. Math. Biol. 51, 616–628, http://dx.doi.org/10.1187/cbe.10-08-0099.

Fraser, C., Donnelly, C.A., Cauchemez, S., Hanage, W.P., Kerkhove, M.D.V., Hollingsworth, T.D., Griffin, J., Baggaley, R.F., Jenkins, H.E., Lyons, E.J., Jombart, T., Hinsley, W.R., Grassly, N.C., Balloux, F., Ghani, A.C., Ferguson, N.M., Rambaut, A., Pybus, O.G., Lopez-Gatell, H., Alpuche-Aranda, C.M., Chapela, I.B., Zavala, E.P., Guevara, D.M.E., Checchi, F., Garcia, E., Hugonnet, S., Roth, C., 2009. T.W.R.P.A. Collaboration, 2009. Pandemic potential of a strain of influenza A (H1N1): early findings. Science 324, 1557–1561, http://dx.doi.org/10.1126/science.1176062.

Ghosh, M., Pugliese, A., 2004. Seasonal population dynamics of ticks, and its influence on infection transmission: a semi-discrete approach. Bull. Math. Biol. 66, 1659–1684, http://dx.doi.org/10.1016/j.bulm.2004.03.007.

Githeko, A.K., Lindsay, S.W., Confalonieri, U.E., Patz, J.A., 2000. Climate change and vector-borne diseases: a regional analysis. Bull. WHO 78, 1136–1147, http://dx.doi.org/10.1590/S0042-96862000000900009.

Gumel, A., Ruan, S., Day, T., Watmough, J., van den Driessche, P., Gabrielson, D., Bowman, C., Alexander, M.E., Ardal, S., Wu, J., Sahai, B.M., 2004. Modeling strategies for controlling SARS outbreaks based on Toronto, Hong Kong, Singapore and Beijing experience. Proc. R. Soc. London 271, 2223–2232, http://dx.doi.org/10.1098/rspb.2004.2800.

Hale, J.K., 1980. Ordinary Different Equations, 2nd ed Krieger.

Hartemink, N.A., Randolph, S.E., Davis, S.A., Heesterbeek, J.A.P., 2008. The basic reproduction number for complex disease systems: defining $R(0)$ for tick-borne infections. Am. Nat. 171, 743–754, http://dx.doi.org/10.1086/587530.

Hartemink, N.A., Purse, B.V., Meiswinkel, R., Brown, H.E., de Koeijer, A., Elbers, A.R., Boender, G.J., Rogers, D.J., Heesterbeek, J.A.P., 2009. Mapping the basic reproduction number (R_0) for vector-borne diseases: a case study on bluetongue virus. Epidemics 1, 153–161, http://dx.doi.org/10.1016/j.epidem.2009.05.004.

Hartemink, N., Vanwambeke, S.O., Heesterbeek, H., Rogers, D., Morley, D., Pesson, B., Davies, C., Mahamdallie, S., Ready, P., 2011. Integrated mapping of establishment risk for emerging vector-borne infections: a case study of canine leishmaniasis in southwest France. PLoS One 6, e20817, http://dx.doi.org/10.1371/journal.pone.0020817.

IPCC, Climate Change, 2001. Third Assessment Report of the Intergovernmental Panel on Climate Change (WG I and II)). Cambridge University Press, Cambridge.

Klich, M., Lankester, M.W., Wu, K.W., 1996. Spring migratory birds (Aves) extend the northern occurrence of blacklegged tick (Acari:Ixodidae). J. Med. Entomol. 33, 581–585.

Leighton, P.A., Koffi, J.K., Pelcat, Y., Lindsay, L.R., Ogden, N.H., 2012. Predicting the speed of tick invasion: an empirical model of range expansion for the Lyme disease vector *Ixodes scapularis* in Canada. J. Appl. Ecol. 49, 457–464, http://dx.doi.org/10.1111/j.1365-2664.2012.02112.x.

Lindsay, L.R. 1995. Factors Limiting the Density of the Black-Legged Tick, *Ixodes scapularis*, in Ontario, Canada. Ph.D. Thesis. University of Guelph.

Lindsay, L.R., Barker, I.K., Surgeoner, G.A., McEwen, S.A., Gillespie, T.J., Addison, E.M., 1998. Survival and development of the different life stages of *Ixodes scapularis* (Acari: Ixodidae) held within four habitats on Long Point, Ontario, Canada. J. Med. Entomol. 35, 189–199.

Marino, S., Hogue, I.B., Ray, C.J., Kirschner, D.E., 2008. A methodology for performing global uncertainty and sensitivity analysis in systems biology. J. Theor. Biol. 254, 178–196, http://dx.doi.org/10.1016/j.jtbi.2008.04.011.

Mckay, M.D., Beckman, R.J., Conover, W.J., 1979. Comparison of 3 methods for selecting values of input variables in the analysis of output from a computer code. Technometrics 21, 239–245.

Morshed, M.G., Scott, J.D., Banerjee, S.N., Banerjee, M., Fitzgerald, T., Fernando, K., Mann, R., Isaac-Renton, J., 1999. First isolation of Lyme disease spirochete, *Borrelia burgdorferi*, from blacklegged tick, *Ixodes scapularis*, removed from a bird in Nova Scotia, Canada. Can. Commun. Dis. Rep. 25, 153–155.

Mount, G.A., Haile, D.G., 1989. Computer simulation of population dynamics of the American dog tick (Acari: Ixodidae). J. Med. Entomol. 26, 60–76.

Mount, G.A., Haile, D.G., Daniels, E., 1997. Simulation of blacklegged tick (Acari:Ixodidae) population dynamics and transmission of *Borrelia burgdorferi*. J. Med. Entomol. 34, 461–484.

Norman, R., Bowers, R.G., Begon, M., Hudson, P.J., 1999. Persistence of tick-borne virus in the presence of multiple host species: tick reservoirs and parasite mediated competition. J. Theor. Biol. 200, 111–118, http://dx.doi.org/10.1006/jtbi.1999.0982.

Ogden, N.H., Lindsay, L.R., Beauchamp, G., Charron, D.F., Maarouf, A., O'Callaghan, C.J., Waltner-Toews, D., Barker, I.K., 2004. Investigation of relationships between temperature and developmental rates of tick *Ixodes scapularis* (Acari: Ixodidae) in the laboratory and field. J. Med. Entomol. 41, 622–633.

Ogden, N.H., Bigras-Poulin, M., O'Callaghan, C.J., Barker, I.K., Lindsay, L.R., Maarouf, A., Smoyer-Tomic, K.E., Waltner-Toews, D., Charron, D.F., 2005. A dynamic population model to investigate effects of climate on geographic range and seasonality of the tick *Ixodes scapularis*. Int. J. Parasitol. 35, 375–389, http://dx.doi.org/10.1016/j.ijpara.2004.12.013.

Ogden, N.H., Maarouf, A., Barker, I.K., Bigras-Poulin, M., Lindsay, L.R., Morshed, M.G., O'Callaghan, C.J., Ramay, F., Waltner-Toews, D., Charron, D.F., 2006. Climate change and the potential for range expansion of the Lyme disease vector Ixodes

scapularis in Canada. Int. J. Parasitol. 36, 63–70, http://dx.doi.org/10.1016/j.ijpara.2005.08.016.

Ogden, N.H., Barker, I.K., Beauchamp, G., Brazeau, S., Charron, D.F., Maarouf, A., Morshed, M.G., O'Callaghan, C.J., Thompson, R.A., Waltner-Toews, D., Waltner-Toews, M., Lindsay, L.R., 2006a. Investigation of ground level and remote-sensed data for habitat classification and prediction of survival of *Ixodes scapularis* in habitats of southeastern Canada. J. Med. Entomol. 43, 403–414, http://dx.doi.org/10.1603/0022-2585(2006)043[0403:IOGLAR]2.0.CO;2.

Ogden, N.H., Bigras-Poulin, M., O'callaghan, C.J., Barker, I.K., Kurtenbach, K., Lindsay, L.R., Charron, D.F., 2007. Vector seasonality, host infection dynamics and fitness of pathogens transmitted by the tick *Ixodes scapularis*. Parasitology 134, 209–227, http://dx.doi.org/10.1017/S0031182006001417.

Ogden, N.H., Lindsay, L.R., Hanincová, K., Barker, I.K., Bigras-Poulin, M., Charron, D.F., Heagy, A., Francis, C.M., O'Callaghan, C.J., Schwartz, I., Thompson, R.A., 2008a. Role of migratory birds in introduction and range expansion of *Ixodes scapularis ticks* and of *Borrelia burgdorferi* and *Anaplasma phagocytophilum* in Canada. Appl. Environ. Microbiol. 74, 1780–1790, http://dx.doi.org/10.1128/AEM.00857-08.

Ogden, N.H., St-Onge, L., Barker, I.K., Brazeau, S., Bigras-Poulin, M., Charron, D.F., Francis, C.M., Heagy, A., Lindsay, L.R., Maarouf, A., Michel, P., Milord, F., O'Callaghan, C.J., Trudel, L., Thompson, R.A., 2008b. Risk maps for range expansion of the Lyme disease vector, *Ixodes scapularis* in, Canada now and with climate change. Int. J. Health Geogr. 22, 7–24, http://dx.doi.org/10.1186/1476-072X-7-24.

Ogden, N.H., Lindsay, L.R., Morshed, M., Sockett, P.N., Artsob, H., 2008c. The rising challenge of Lyme borreliosis in Canada. Can. Commun. Dis. Rep. 34, 1–19.

Ogden, N.H., Lindsay, L.R., Morshed, M., Sockett, P.N., Artsob, H., 2009. The emergence of Lyme disease in Canada. Can. Med. Assoc. J. 180, 1221–1224, http://dx.doi.org/10.1503/cmaj.080148.

Ogden, N.H., Bouchard, C., Kurtenbach, K., Margos, G., Lindsay, L.R., Trudel, L., Nguon, S., Milord, F., 2010. Active and passive surveillance and phylogenetic analysis of *Borrelia burgdorferi* elucidate the process of Lyme disease risk emergence in Canada. Environ. Health Perspect. 118, 909–914, http://dx.doi.org/10.1289/ehp.0901766.

Parmesan, C., Yohe, G., 2003. A globally coherent fingerprint of climate change impacts across natural systems. Nature 421, 37–42, http://dx.doi.org/10.1038/nature01286.

Porco, T.C., 1999. A mathematical model of the ecology of Lyme disease. Math. Med. Biol. 126, 261–296, http://dx.doi.org/10.1093/imammb/16.3.261.

Randolph, S.E., Miklisova, D., Lysy, J., Rogers, D.J., Labuda, M., 1999. Incidence from coincidence: patterns of tick infestations on rodents facilitate transmission of tick-borne encephalitis virus. Parasitology 118, 177–186.

Rosá, R., Pugliese, A., 2007. Effects of tick population dynamics and host densities on the persistence of tick-borne infections. Math. Biosci. 208, 216–240, http://dx.doi.org/10.1016/j.mbs.2006.10.002.

Rosá, R., Pugliese, A., Norman, R., Hudson, P.J., 2003. Thresholds for disease persistence in models for tick-borne infections including non-viraemic transmission, extended feeding and tick aggregation. J. Theor. Biol. 224, 359–376, http://dx.doi.org/10.1016/S0022-5193(03)00173-5.

Schmidt, K.A., Ostfeld, R.S., 2001. Biodiversity and the dilution effect in disease ecology. Ecology 82, 609–619, http://dx.doi.org/10.1890/0012-9658(2001)082[0609:BATDEI]2.0.CO;2.

Smith, D.L., McKenzie, F.E., Snow, R.W., Hay, S.I., 2007. Revisiting the basic reproductive number for malaria and its implications for malaria control. PLoS Biol. 5, e42, http://dx.doi.org/10.1371/journal.pbio.0050042.

The malERA Consultative Group on Modeling. 2011. A Research Agenda for Malaria Eradication: Modeling. PLoS Med. 8, e1000403. http://dx.doi.org/10.1371/journal.pmed.1000403.

Wang, W., Zhao, X.-Q., 2008. Threshold dynamics for compartmental epidemic models in periodic environments. J. Dyn. Diff. Equat. 20, 699–717, http://dx.doi.org/10.1007/s10884-008-9111-8.

Webb, G., Blaser, M., Zhu, H., Ardal, S., Wu, J., 2004. Critical role of nosocomial transmission in the Toronto SARS outbreak. Math. Biosci. Eng. 1, 1–13.